High Plasticity and Substantial Deformation in Nanocrystalline NiFe Alloys Under Dynamic Loading

By *Sheng Cheng,* Yonghao Zhao,* Yazhou Guo, Ying Li, Qiuming Wei, Xun-Li Wang, Yang Ren, Peter K. Liaw, Hahn Choo,* and *Enrique J. Lavernia*

Bulk nanocrystalline (NC) materials (with an average grain size <100 nm) have been widely reported to exhibit high strength but disappointingly low plasticity. In this Communication, upon dynamically deforming an NC NiFe alloy, we report impressively large plastic deformation: from 8% quasi-static strain to a maximum prescribed dynamic strain of ~22% without failure. This large, dynamic plastic deformation is accompanied by a much elevated yield strength (33% increase compared with quasi-static strength). Detailed postmortem microstructure analysis reveals that the dynamic deformation resulted in significant grain coarsening and de-twinning manifested by a great reduction of the twin density vis-à-vis slight grain coarsening without de-twinning in quasi-static deformation. We envisage that such mechanisms are responsible for the unique texture as compared with the conventional deformation texture as uncovered by in-depth texture analysis based on X-ray diffraction (XRD) using synchrotron radiation. Our efforts highlight potential ingenious avenues to exploit the superior behavior of NC materials under extreme conditions by invoking the favorable deformation mechanisms, such as reported herein.

In recent years, bulk NC metals and alloys have attracted a great deal of attention as potential candidates for next-generation high-strength materials. Indeed, success has been achieved on the strength improvement with grain refinement to nanometer scale, extending from the well-known Hall–Petch relation to at least ~20 nm.[1–3] However, often it appears that the increased strength is at the expense of the capability of the materials to sustain plastic deformation. In fact, poor ductility associated with NC materials has become a seemingly insurmountable obstacle for their widespread technological applications.[4,5] Most of the recently developed strategies for improving tensile ductility have been limited to ultrafine grained materials (with an average grain size >100 nm) with a dislocation-dominated plastic deformation mechanism,[6–11] which may not be applicable to bulk NC materials where grain-boundary-mediated plasticity prevails.[12–14] Although large plastic deformation has been observed in compression of micrometer-sized pillars of NC materials,[15,16] little has been said regarding the deformation mechanism. Therefore, it still remains an open question as to how considerable plastic deformation can be possible in bulk samples of NC materials. Moreover, the application of materials under dynamic loading in many occasions requires a combination of a high resistance to sample yielding and a good tolerance of plastic deformation. In this paper, we provide strong evidence for very large plastic deformation under dynamic loading of bulk NC samples and we also attempt to unravel the underlying deformation mechanism responsible for such behavior via careful and in-depth postmortem microstructural analysis.

NC NiFe alloy samples (Ni-20 wt% Fe) were prepared by pulse electrodeposition. Uniaxial dynamic compression at strain rates of around $10^3\ s^{-1}$ was performed using the Kolsky bar technique with loading direction in the deposition (or thickness) direction. For the purpose of comparison, quasi-static compression tests were carried out at a strain rate of $1 \times 10^{-3}\ s^{-1}$ in the same direction of loading. Microstructural evolutions upon dynamic and quasi-static loading were characterized using synchrotron XRD and transmission electron microscopy (TEM) as well as high-resolution TEM (HRTEM).

Figure 1 shows the true stress–strain curves of the NC NiFe alloy under dynamic and quasi-static loading conditions. The dynamic yield stress approaches ~2 GPa as compared with ~1.5 GPa under quasi-static condition. This translates into ~33% increase in strength upon dynamic loading. More importantly, Figure 1 reveals a remarkably enhanced plasticity of this NC NiFe alloy upon dynamic loading: while the quasi-static specimens fail at ~8% strain, no failure is observed under dynamic loading. It is worth pointing out that dynamic loading was stopped at a prescribed strain. Close examination of the dynamic stress–strain curves also suggests that, although flow softening is present in all the curves, the softening is more or less steady, that is, it proceeds in a uniform manner, and no precipitous stress collapse is observed due to the development of adiabatic shear banding.[17,18] This is further asserted by postmortem examination of the specimens. In contrast, the quasi-static stress–strain curve exhibits an initial hardening

[*] Dr. S. Cheng, Prof. P. K. Liaw, Prof. H. Choo
Department of Materials Science and Engineering
University of Tennessee
Knoxville, TN 37996 (USA)
E-mail: scheng1@utk.edu
Dr. Y. Zhao, Dr. Y. Li, Prof. E. J. Lavernia
Department of Chemical Engineering and Materials Science
University of California
Davis, CA 95616 (USA)
E-mail: yhzhao@ucdavis.edu
Y. Guo, Prof. Q. Wei
Department of Mechanical Engineering
University of North Carolina
Charlotte, NC 28223 (USA)
Dr. X.-L. Wang
Neutron Scattering Science Division
Oak Ridge National Laboratory
Oak Ridge, TN 37831 (USA)
Dr. Y. Ren
Advanced Photon Source, Argonne National Laboratory
Argonne, IL 60439 (USA)

DOI: 10.1002/adma.200901991

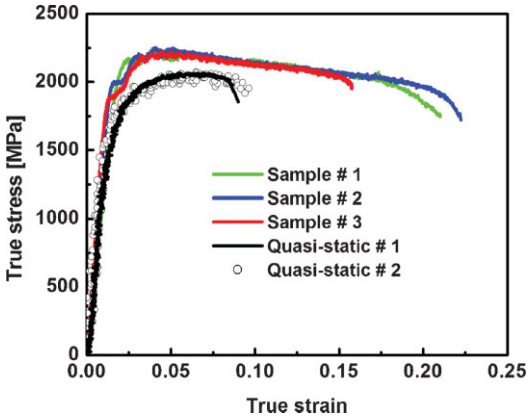

Figure 1. Dynamic and quasi-static true stress–strain curves of the NC NiFe alloy. Three samples were used for the dynamical tests with strain rates ranging from 1×10^3 to 3×10^3 s^{-1}. Significantly enhanced dynamic deformation strain and strength were observed compared to the quasi-static loading with a strain rate of 1×10^{-3} s^{-1}. It should be noted that none of the dynamic specimens failed. The dynamic loading was discontinued at a prescribed strain level. Although dynamic flow softening is persistent in the dynamic strain–stress curves, no precipitous load drop is observed before the prescribed strain, indicative of nearly uniform deformation and absence of plastic instability such as adiabatic shear banding.[17,18]

followed by quick saturation of the flow stress and final premature failure. In order to study the microstructure evolution associated with the dynamic deformation, we interrupted one of the tests (Sample #3) at an early strain and subsequent reloading of this sample showed very similar stress–strain behavior in terms of strength and flow softening.

Postmortem synchrotron XRD did not reveal any new phase upon dynamic loading but it did suggest texture evolution in the NC NiFe alloy during dynamic deformation. Figure S1 in the Supporting Information displays the pole figures of both the as-received material and the specimen subjected to dynamic deformation. A weak (200) texture is detected in the deposition direction of the as-received material, which is the typical growth texture associated with electrodeposition of face-centered cubic (fcc) metals and alloys. Dynamic deformation has intensified the previously weak (200) texture but the {110} and {111} orientations have become randomly distributed. Such texture evolution in the NC NiFe alloy upon dynamic loading is different from the conventional route of texture development established in coarse-grained fcc polycrystalline metals, where as a result of dislocation slip a (110) texture develops preferentially in the loading direction under uniaxial compression.[19] This novel texture evolution in the NC NiFe alloy under dynamic deformation points to new deformation mechanisms beyond merely dislocation slips. Detailed TEM analysis provided in the following verifies such surmise.

To understand the peculiar dynamic deformation behavior of the NC NiFe alloy, we have performed extensive TEM and HRTEM analyses of both the as-received and the dynamically and quasi-statically deformed samples. Considering the presence of the deposition as well as the deformation texture, the TEM and HRTEM characterizations were conducted in both top view (electron beam parallel to deposition direction) and side view (electron beam normal to the deposition direction). Representative microstructures of the as-received NC NiFe sample from the two viewing directions are shown in Figure 2. Equi-axed grains with sizes from ~5 to 60 nm were observed in the top view (Fig. 2a). Statistics from ~360 grains indicate that most of the grains fall in the range between 10 and 20 nm (Fig. 2e). Some columnar grains were observed in side view (Fig. 2b). Close examination reveals high-density growth twins in side view, which are nearly invisible in top view. Both top-view and side-view TEM analysis suggest random grain orientations with sharp large-angle boundaries, as confirmed by the nearly continuous ring patterns of selected-area diffraction (SAD; insets of Fig. 2a and b), taken from an area of ~500 nm in diameter. Statistic TEM observations indicate that the above microstructural characteristics are exhibited in the whole sample, as shown in Figure S2 at low magnification. HRTEM shows that some small grains may contain a few dislocations (Fig. 2c and Fig. S3a), while others are dislocation-free (Fig. S3b and c). Figure 2d reveals the detailed structure of growth twins in two neighboring grains, G1 and G2, where parallel twin boundaries (TBs) can be seen. These observations are similar to other studies.[20]

Upon dynamic deformation, the peak of the grain size distributions clearly shifts to large values (Fig. 2f). The average grain sizes increase from 19 to 36 nm in side view and from 18 to 35 nm in top view. In contrast, the quasi-statically deformed specimen has much less grain growths (Fig. S4) with average grain sizes of 23 nm (top view) and 21 nm (side view). Despite the increase of overall grain sizes, some small grains still remain between 5 and 10 nm after the dynamic deformation, though with reduced population in both top and side views. HRTEM observations show that the dislocation configuration (in terms of density and structure) in these small grains remains almost unchanged (Fig. S5). Moreover, neither the average grain size nor the grain shape seem to have changed in these small grains. This may be taken as indirect evidence that plastic deformation, if any, of such small grains may be mediated by grain-boundary activities. This is in line with numerous computer simulations, which suggest that grains of such small size could accommodate plastic deformation by grain-boundary sliding.[13,14,21] In addition, we have observed marked structural features in the relatively large grains (>60 nm) after dynamic loading (Fig. 3a). Detailed TEM reveals that many of the large grains exhibit irregular shape and are composed of two or more subgrains (labeled from G1 to G4 in Fig. 3a). Figure S6 serves as another representative example in which roughly six subgrains (labeled from G1 to G6) can be discerned within a large grain of ~200 nm. These subgrains are of size <50 nm. The SAD ring patterns become less continuous (inset of Fig. 3a) than those from the as-deposited sample, a consequence of grain coarsening. The large grains appear to come about through coalescence of small grains. It is likely that the coalescence occurs when two grains with close orientations make contact during the course of grain sliding. Grain coalescence could also be assisted by rotation of neighboring grains, which eventually merge into a single grain.[12,22] Agglomeration of smaller grains to form larger ones will naturally diminish the populations of the former. Such grain-growth mechanism, encountered herein, is in fact in excellent agreement with a recent in situ TEM study of NC Al, where initially separated grains with similar orientation can be combined.[23] Grain coalescence can sometimes be found in the quasi-static samples but the extent is much less than that

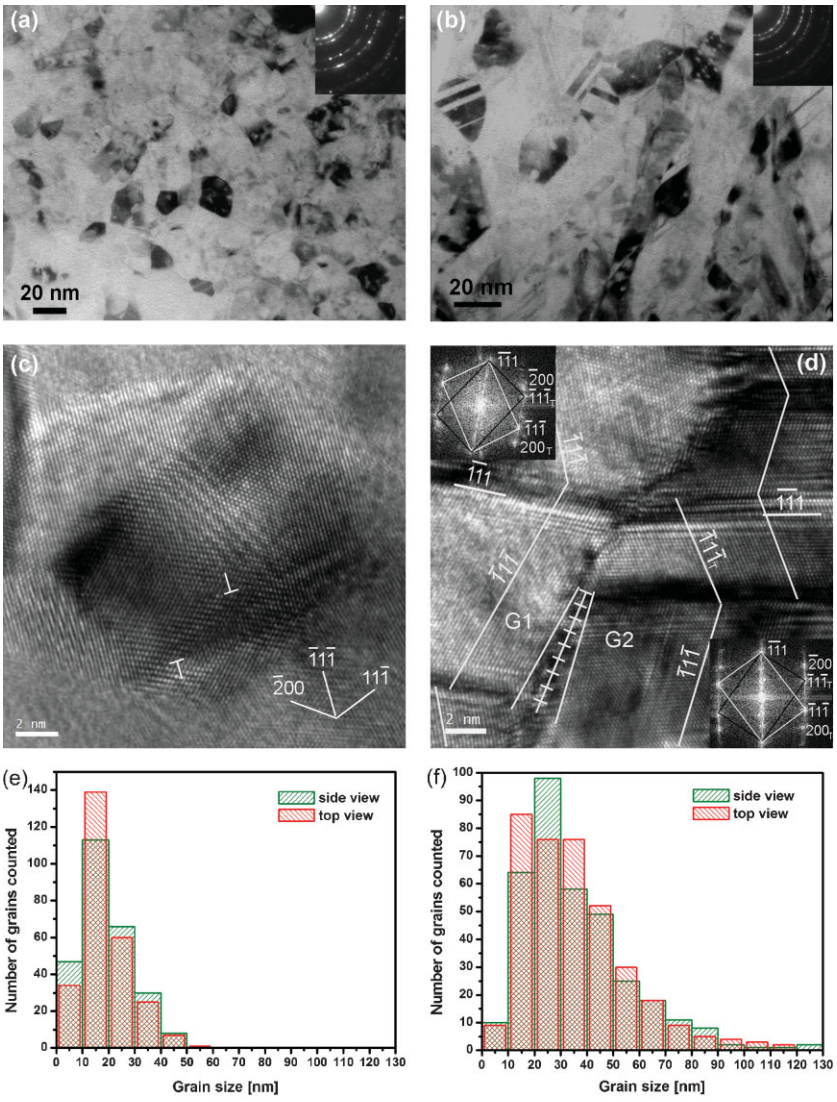

Figure 2. a,b) Representative bright-field TEM and c,d) HRTEM images of the as-received NC NiFe alloy in top view (a) and side view (b–d). e,f) Grain-size distributions before and after the dynamic deformation, respectively. The insets in (a) and (b) are SAD patterns from an area with a diameter of about 500 nm. HRTEM images were taken from a ⟨011⟩ zone axis. Dislocations in a small grain in (c) are marked by "T". The insets in (d) are diffraction patterns from grains G1 and G2 showing twin relationship. Small-angle grain boundary between G1 and G2 is formed by dislocation. About 360 grains each were counted for both side view and top view.

observed in dynamically deformed samples. The large grains in the quasi-static specimen are often observed to have two dark neighboring grains sharing a small-angle boundary (Fig. S7).

In addition to the top-view TEM observations, indicative of grain growth via coalescence of small grains, a similar mechanism is also commonly observed in side view, as shown in Figure 3b for a dynamically deformed sample. Here, again, large grains embracing many sub-grains can be clearly witnessed, accompanied by the less continuous SAD ring pattern. More interestingly, our TEM observations suggest that many preexisting growth twins have disappeared upon dynamic deformation. This is strong evidence for a new deformation mechanism in this NC NiFe alloy namely de-twinning. Statistics indicate that the dynamic deformation has resulted in a reduction of twin density from 1.54×10^{-4} to 4.36×10^{-5} nm^{-2}, while quasi-static deformation has not altered the twin density evidently (Fig. S8). To further understand the de-twinning process, we searched extensively for the debris of twins by both TEM and HRTEM. Figure 3c presents a scenario where TBs have been shifted (pointed by black arrow) and partly eliminated (pointed by white arrow, the twins T1 and T2 have been taken over by a grain T). In other cases, the TBs are severely distorted (Fig. S9). Figure 3d shows an HRTEM image to reveal the distorted and shifted TBs. In contrast to the as-received specimen, a high density of dislocation is found near the TBs (Fig. S10). Even though the exact process is not clear without in situ observation, it appears that the de-twinning process involves the contribution from partial dislocation activity. Mechanical annealing of TBs such as evidenced in Figure 3b–d leads to an increased average twin width and, at the same time, to a decreased twin density. In addition, bearing in mind that de-twinning can induce a drastic orientation change, we may regard de-twinning to be the primary mechanism responsible for the texture change during dynamic loading of this NC NiFe alloy.

A natural concern arises regarding the possible grain growth and de-twinning induced by the adiabatic temperature rise common in dynamic loading of visco-plastic materials. The overall estimated adiabatic temperature rise within the sample during dynamic loading is less than 80 K (Supporting Information), thus, insubstantial for significant grain growth and de-twinning of the NC NiFe alloy. Hence, we do not consider adiabatic temperature rise to be the primary contributing factor leading to the grain-growth and de-twinning processes. Similar to Reference [24] we hold the view that such microstructure evolutions are mechanically driven.

Comparing with the quasi-static deformation, the high strength and respectable dynamic plastic deformation observed in the NC NiFe alloy are, thus, closely related to the peculiar deformation mechanisms. Several factors may contribute to the increased strength and plasticity. First, the high strain rate associated with dynamic loading could enhance the yield stress. Previous studies have suggested that the strain-rate sensitivity in fcc metals increases as grain size reduces and such rate effect can become substantial for NC metals.[25,26] The much increased strain rate sensitivity also helps to suppress plastic instability, which explains the absence of precipitous stress collapse in the dynamic stress–strain curves of such strong NC metals (such stress collapse is usually a signature of adiabatic shear banding in the specimen). The post-yielding decrease in flow stress might be caused by gradual grain coarsening and de-twinning, as well as the homogeneous and gradual adiabatic temperature rise when

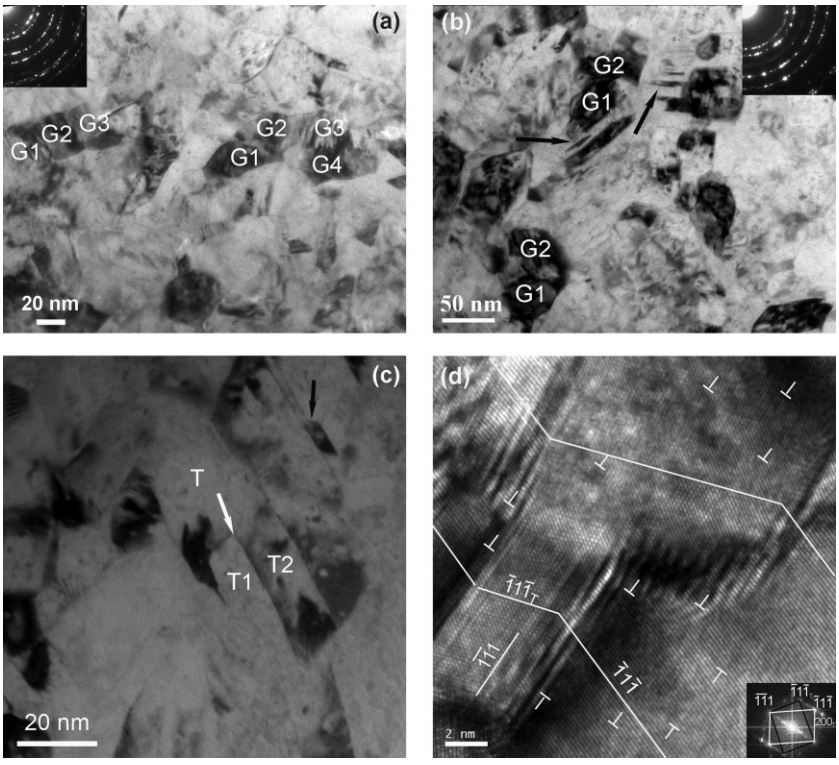

Figure 3. Postmortem bright-field TEM images of the NC NiFe alloy after dynamic deformation from both top (a) and side (b) views. Large grains are found to be composed of several subgrains labeled from G1 to G4. The black arrows in (b) point to some twin debris. c) Magnified TEM image on the twin debris from side view. The TB marked by the white arrow has partly retreated from its original position and the TB marked by the black arrow has shifted, suggesting the de-twinning process. d) HRTEM image of the twin debris from side view. The inset is a Fourier transformation showing twin relationship. The TB is shifted and distorted.

dynamic deformation proceeds. Preexisting twins have been reported to enhance tensile ductility at quasi-static loading rates by the much increased strain hardening and strain rate hardening in NC fcc metals, such as Cu, due to dislocation–TB interactions.[7] However, in dynamic compression, as in our study, the compressive ductility is determined by the crack initiation and catastrophic crack propagation as a consequence of adiabatic shear banding. We believe that in our samples the primary role of de-twinning and grain rotation is to relieve the stress concentrations that may also serve as triggers of adiabatic shear banding. This, in turn, increases the compressive ductility of the sample. Absence of plastic instability under compressive loading of our samples due to the aforementioned reasons allows us to achieve a large ultimate plastic strain without failure.

In summary, under dynamic loading a NC NiFe alloy showed both higher strength and higher plasticity than under quasi-static loading. Our elaborate analyses suggest that the dynamic plastic deformation of the NC NiFe alloy is mediated by processes such as de-twinning, grain-boundary sliding, and grain coarsening through grain coalescence. The impressively increased dynamic plasticity observed in this work can be primarily attributed to the deformation mechanism of de-twinning and grain coarsening. The de-twinning mechanism, in particular, seems to be a unique deformation mechanism under dynamic loading for this NC alloy.

An Experimental Section is provided in the Supporting Information.

Acknowledgements

S.C. and Y.Z. contributed equally to this work. S.C. and P.K.L. acknowledge financial support by the NSF International Materials Institutes program (DMR-0231320) and NSF Major Research Instrumentation Program (DMR-0421219). Y.Z. and E.J.L. acknowledge support by the Office of Naval Research (Grant number ONR N00014-08-1-0405). X.-L.W. acknowledges support by US Department of Energy (DE-AC05-00OR22725 and DE-AC02-06CH11357) with UT-Battelle, LLC. Supporting Information is available online from Wiley InterScience or from the authors.

Received: June 13, 2009
Published online: October 2, 2009

[1] J. R. Weertman, in *Nanostructured Materials: Processing, Properties and Applications*, 2nd ed. (Eds: C. C. Koch, G. E. McGuire, S. M. Rossnagel, R. F. Bunshah), William Andrews Publishing, Norwich, New York **2007**, p. 537.
[2] K. M. Youssef, R. O. Scattergood, K. L. Murty, J. A. Horton, C. C. Koch, *Appl. Phys. Lett.* **2005**, *87*, 091904.
[3] K. S. Kumar, S. Suresh, M. F. Chisholm, J. A. Horton, P. Wang, *Acta Mater.* **2003**, *51*, 387.
[4] C. C. Koch, D. G. Morris, K. Lu, A. Inoue, *MRS Bull.* **1999**, *24*, 54.
[5] a) C. C. Koch, *Scr. Mater.* **2003**, *49*, 657. b) E. Ma, *Scr. Mater.* **2003**, *49*, 663.
[6] C. C. Koch, K. M. Youssef, R. O. Scattergood, K. L. Murty, *Adv. Eng. Mater.* **2005**, *7*, 787.
[7] E. Ma, *JOM* **2006**, *58*, 49.
[8] Y. Wang, M. Chen, F. Zhou, E. Ma, *Nature* **2002**, *419*, 912.
[9] Y. H. Zhao, T. Topping, J. F. Bingert, A. M. Dangelewicz, Y. Li, W. Liu, Y. T. Zhu, Y. Z. Zhou, E. J. Lavernia, *Adv. Mater.* **2008**, *18*, 3028.
[10] L. Lu, X. Chen, X. Huang, K. Lu, *Science* **2009**, *323*, 607.
[11] Y. H. Zhao, J. F. Bingert, Y. T. Zhu, X. Z. Liao, R. Z. Valiev, Z. Horita, T. G. Langdon, Y. Z. Zhou, E. J. Lavernia, *Appl. Phys. Lett.* **2008**, *92*, 081903.
[12] Z. W. Shan, E. A. Stach, J. M. K. Wiezorek, J. A. Knapp, D. M. Follstaedt, S. X. Mao, *Science* **2004**, *305*, 654.
[13] H. Van Swygenhoven, P. A. Derlet, *Phys. Rev. B* **2001**, *64*, 224105.
[14] J. Schiøtz, F. D. Di Tolla, K. W. Jacobsen, *Nature* **1998**, *391*, 561.
[15] D. Pan, S. Kuwano, T. Fujita, M. W. Chen, *Nano Lett.* **2007**, *7*, 2108.
[16] N. A. Mara, D. Bhattacharyya, P. Dickerson, R. G. Hoagland, A. Misra, *Appl. Phys. Lett.* **2008**, *92*, 231901.
[17] Q. Wei, L. Kecskes, T. Jiao, K. T. Hartwig, K. T. Ramesh, E. Ma, *Acta Mater.* **2004**, *52*, 1859.
[18] Q. Wei, H. T. Zhang, B. E. Schuster, K. T. Ramesh, R. Z. Valiev, L. J. Kecskes, R. J. Dowding, L. Magness, K. Cho, *Acta Mater.* **2006**, *54*, 4079.
[19] K. X. Tao, D. W. Brown, S. C. Vogel, H. Choo, *Metall. Mater. Trans. A* **2006**, *37*, 3469.
[20] Y. B. Wang, J. C. Ho, Y. Cao, X. Z. Liao, H. Q. Li, Y. H. Zhao, E. J. Lavernia, S. P. Ringer, Y. T. Zhu, *Appl. Phys. Lett.* **2009**, *94*, 091911.
[21] J. Schiotz, K. W. Jacobsen, *Science* **2003**, *301*, 1357.
[22] Y. B. Wang, J. C. Ho, X. Z. Liao, H. Q. Li, S. P. Ringer, Y. T. Zhu, *Appl. Phys. Lett.* **2009**, *94*, 011908.
[23] M. Legros, D. S. Gianola, K. J. Hemker, *Acta Mater.* **2008**, *56*, 3380.
[24] K. Zhang, J. R. Weertman, J. A. Eastman, *Appl. Phys. Lett.* **2005**, *87*, 061921.
[25] S. Cheng, E. Ma, Y. M. Wang, L. J. Kecskes, K. M. Youssef, C. C. Koch, U. P. Trociewitz, K. Han, *Acta Mater.* **2005**, *53*, 1521.
[26] Q. Wei, S. Cheng, K. T. Ramesh, E. Ma, *Mater. Sci. Eng.* **2004**, *381*, 71.